An in Situ Time-Dependent Study of CO Oxidation on Pt(111) in Aqueous Solution by Voltammetry and Sum Frequency Generation

Keng C. Chou,[†,‡] Nenad M. Markovic,[‡] Joonyeong Kim,[†,‡] Philip N. Ross,[‡] and Gabor A. Somorjai*[,†,‡]

Departments of Chemistry, University of California, Berkeley, California 94720, and Materials Science Division, Lawrence Berkeley National Laboratory, Berkeley, California 94720

Received: October 17, 2002; In Final Form: December 15, 2002

In situ time-dependent measurements using voltammetry and sum frequency generation (SFG) were carried out to study CO oxidation on a Pt(111) electrode. The scan-rate dependence of CO oxidation was measured by changing the scan rate from 50 to 0.5 mV/s. While the basic shape of the CO stripping curves was unaffected by sweep rate, the oxidation potential of CO was lowered by 0.1 V, from 0.84 to 0.74 V. The measurements of SFG spectra and CO stripping were carried out simultaneously to clarify the discrepancy between SFG and CO stripping measurements reported in earlier SFG studies. Our results showed that the SFG peak attributed to the CO stretch vanished immediately after the CO stripping current reached its maximum value. In the preignition potential region, the frequency shift of the CO stretch observed by SFG agrees with that observed by IR spectroscopy. Additionally, in the ignition potential region, a significant blue shift of CO stretching frequency was observed. For the first time, a 360% enhancement of SFG intensity coinciding with the red shift of stretching frequency was observed in the preignition potential region. While it was not observed by IR spectroscopy, it shows similar behavior to limited Raman spectroscopy measurements obtained from a roughened Pt surface.

Introduction

There is a great deal of interest in understanding the mechanism whereby adsorbed CO undergoes electrochemical oxidation to CO_2.[1−8] In particular, the electro-oxidation of CO on well-defined electrodes may lead to a better understanding of the oxidation process and could result in the design of new catalysts.[9] CO oxidation on platinum electrodes has been extensively studied using infrared reflection absorption spectroscopy (IRAS),[2,10,11] scanning tunneling microscopy/atomic force microscopy (STM/AFM),[12,13] surface X-ray diffraction (SXD),[14] and sum frequency generation (SFG).[15,16] Although a Langmuir−Hinshelwood type adsorbate−adsorbate reaction is generally accepted, the mechanism for the electrochemical oxidation of adsorbed CO in solutions is not clearly understood. It is assumed that CO and another oxygen-containing surface species, presumably OH_{ads}, form CO_2.

Previously, Weaver et al. found that the IR spectra showed two peaks in the hydrogen underpotential deposition (UPD) region with the presence of CO in solution: a predominate sharp peak at 2066 cm^{-1}, which is attributed to atop coordinated CO, and a weaker peak centered at 1773 cm^{-1}, assigned to CO adsorbed at the 3-fold hollow sites.[10] By increase of the potential above 0.25 V (vs reversible hydrogen electrode (RHE)), the atop peak was broadened and the peak at 1773 cm^{-1} was replaced by a peak at 1850 cm^{-1}, which is commonly assigned to bridge-bonded CO. Studies using STM showed a p(2 × 2)−3CO adlayer with a coverage of $\theta_{CO} = 0.75$ monolayer in near-saturated CO solution at 0.05 V and a transition to a ($\sqrt{19}\times\sqrt{19}$)-R23.4° adlayer with $\theta_{CO} = 0.68$ mL at $V > 0.2$ V.[13] Another CO adlayer structure, having a ($\sqrt{7} \times \sqrt{7}$)R19.7° cell ($\theta_{CO} = 0.57$ mL), was commonly observed for the irreversibly adsorbed CO over the potential range of 0.05−0.45 V after the removal of CO in the solution. On the other hand, studies using SXD showed that p(2×2)−3CO is the only structure, which has long-range order.[14]

Recently, SFG has been used to study CO oxidation on Pt-(111) in CO-free 0.5 M H_2SO_4 aqueous electrolyte[15] and in CO-saturated 0.1 M $HClO_4$ aqueous electrolyte.[16] These studies reported a discrepancy between the CO oxidation potential measured by voltammetry and the disappearance of SFG signal: The SFG signal of CO disappears at a potential between 0.45 and 0.55 V, which is well below the CO oxidation potential (0.75−0.85 V) observed in CO stripping curves. However, in these experiments, each SFG spectrum at a given potential was acquired in 20−60 min, while the CO stripping measurements scanned through the entire potential range in less than a minute. In this paper, we measured the potential scan rate dependence of the CO oxidation. While the oxidation potential of CO is dependent on the scan rate, the shape of the CO stripping curve stays mostly unchanged. When the scan rate was decreased from 50 to 0.5 mV/s, the oxidation potential was lowered by 0.1 V, from 0.84 to 0.74 V. Therefore, simultaneous measurements of the SFG spectra and the CO stripping current are essential, if a meaningful comparison between the two techniques is desired. Our measurements show that, if measured simultaneously, the SFG spectra and the CO stripping current were consistent: The CO stretch peak vanished immediately after the oxidation current reached its maximum. In the preignition potential region, the observed CO stretching frequency agrees with results observed by IR spectroscopy. In the ignition potential region, a significant blue shift of frequency was observed for the first time. In contrast to IR absorption intensity, we observed a significant enhancement of SFG intensity in the preignition potential region.

* Author to whom correspondence should be addressed. E-mail: somorjai@socrates.berkeley.edu
† University of California, Berkeley
‡ Lawrence Berkeley National Laboratory

10.1021/jp027235c CCC: $25.00 © 2003 American Chemical Society
Published on Web 02/04/2003

Experimental Details

A Nd:YAG laser at 1064 nm with 20 ps pulse width and 20 Hz repetition rate was frequency doubled to 532 nm in a BBO crystal. The tunable IR beam was generated in an $AgGaS_2$ crystal by difference frequency mixing of the 1064 nm beam with the output of a BBO optical parametric generator/amplifier (OPG/OPA) pumped by the 532 nm beam. The 532 nm and IR beams had intensities of 70 and 120 μJ per pulse, respectively. Two laser beams were overlapped both spatially and temporally on the sample at incident angles of 36° and 44°, respectively. The IR beam was focused on the sample and has a spot size of 0.65 mm (full width at half maximum (fwhm)). To minimize the effect of Gaussian beam profile and walk-off of the IR beam during OPG/OPA tuning, a flat top 532 nm beam was imaged onto the sample, yielding an image size of 3.5 mm in diameter. The SFG spectra were normalized against that from a Z-cut quartz crystal.

A Pt(111) single crystal with a thickness of 3 mm and a diameter of 6 mm was used as an electrode. The electrode was prepared by flame annealing the platinum single crystal in a hydrogen/air flame for 5 min and quickly transferred into a glass chamber with flowing high-purity argon gas for approximately 10 min. Then the sample was immediately covered with a drop of water and transferred to an electrochemical cell or spectroscopy cell. A standard calomel electrode (−241 mV vs RHE) was used as the reference electrode. All the potentials referred to in this paper have been converted into potentials with respect to an RHE. The electrolytic solution (0.5 M H_2SO_4) was purged for 30 min with argon before the experiment to remove O_2 from the solution. Voltammetry experiments were carried out in a hanging meniscus electrode configuration, so that only the polished Pt(111) face was in contact with the electrolyte. The sample is considered to be clean when the voltammetry of the platinum electrode displays the characteristic peaks of a clean Pt(111) surface as shown in Figure 1A.[17,18] While the potential was held at 40 mV, CO was adsorbed onto the Pt surface by purging the solution with CO for 10 min and then by purging with Ar for another 30 min to remove residual CO in the solution. In the SFG experiments, the Pt electrode was inserted into a Teflon holder so that only the polished (111) face was in contact with the electrolyte. CO was adsorbed onto the surface for 10 min at 40 mV, and then the CO-saturated solution was replaced with Ar-purged solution while holding the potential at 40 mV. The electrode is then pressed against a CaF_2 window for the SFG experiment. The thin film of electrolyte between the Pt and the window was about 5 μm. The temperature change of the thin water layer introduced by laser irradiation is discussed in the Appendix.

It has been shown that the intensity of SFG is proportional to the absolute square of the surface nonlinear susceptibility[19]

$$I_{\mathrm{SFG}} \propto |\chi_{\mathrm{NR}}^{(2)} + \chi_{\mathrm{R}}^{(2)}|^2 = |\chi_{\mathrm{NR}}^{(2)} + \frac{A_{\mathrm{q}}}{\omega_{\mathrm{IR}} - \omega_{\mathrm{q}} + i\Gamma}|^2 \quad (1)$$

with

$$A_{\mathrm{q},ijk} = N_{\mathrm{s}} \sum_{lmn} a_{\mathrm{q},lmn} \langle (\hat{\imath} \cdot \hat{l})(\hat{\jmath} \cdot \hat{m})(\hat{k} \cdot \hat{n}) \rangle \quad (2)$$

$$a_{\mathrm{q},lmn} = -\frac{1}{2\epsilon_{\mathrm{o}}\omega_{\mathrm{q}}} \frac{\partial \mu_{\mathrm{n}}}{\partial Q_{\mathrm{q}}} \frac{\partial \alpha_{lm}}{\partial Q_{\mathrm{q}}} \quad (3)$$

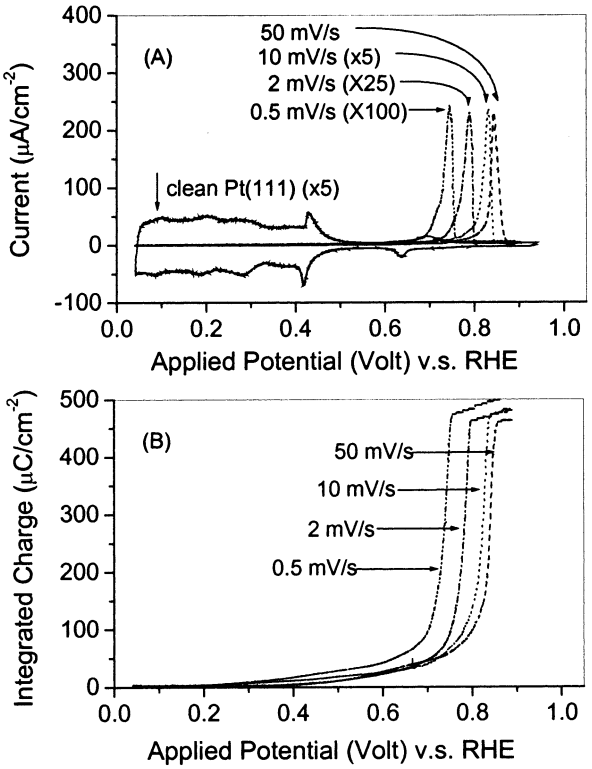

Figure 1. CO stripping current and the integrated charge as a function of applied potential at scan rates of 50, 10, 2, and 0.5 mV/s.

where $\chi_{\mathrm{NR}}^{(2)}$, $\chi_{\mathrm{R}}^{(2)}$, A_{q}, ω_{q}, Γ, $\langle\ \rangle$, $\partial\mu_{\mathrm{n}}/\partial Q_{\mathrm{q}}$, and $\partial\alpha_{\mathrm{lm}}/\partial Q_{\mathrm{q}}$ are the nonresonant contribution, resonant contribution, amplitude, resonant frequency, width, average over orientation distribution, infrared dipole derivative, and Raman polarizability tensor, respectively.

Results and Analysis

Figure 1 shows the measured CO stripping current and the integrated charge as functions of applied potential at scan rates of 50, 10, 2, and 0.5 mV/s. While the CO oxidation potential is dependent on the scan rate, the shape of the CO stripping curves is mostly unchanged. The CO stripping curves can be separated into two potential regions: the preignition and the ignition potential regions.[5,14,20] Approximately 20% of the CO was oxidized in the preignition potential region regardless of the potential sweep rate. They are characterized as a weakly adsorbed state ($CO_{ad,w}$) that oxidized in the preignition potential region and a strongly adsorbed state ($CO_{ad,s}$) that oxidized in the ignition potential region.

To estimate the coverage of CO from the integrated charge, it is necessary to correct the total integrated charge by the contribution from other surface processes that occur after the CO is removed. The total integrated charge during oxidation was 460 μC/cm^2. It was suggested that, in 0.5 M H_2SO_4 solution, the oxidative removal of CO is followed by adsorption of bisulfate anions (~80 μC/cm^2) and adsorption of OH^- (~15 μC/cm^2).[14]

$$\begin{aligned} Q_{\mathrm{CO}} &= Q_{\mathrm{t}} - Q_{\mathrm{HSO_4}} - Q_{\mathrm{OH}} \\ &= 460 - 80 - 15\ (\mu\mathrm{C/cm^2}) \\ &= 365\ (\mu\mathrm{C/cm^2}) \end{aligned}$$

For the two-electron oxidation of CO to CO_2, a monolayer of CO on Pt(111) would produce a charge density of 480 μC/cm^2. Therefore, a charge density of 365 μC/cm^2 corresponds to

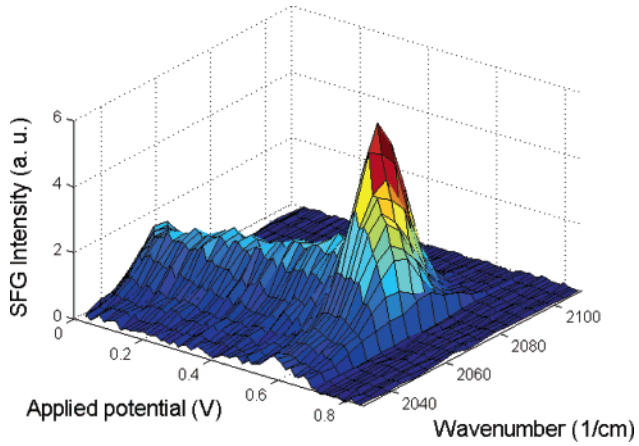

Figure 2. CO vibrational spectra recorded every 22 s during a positive-going potential sweep at 0.5 mV/s.

a coverage of 0.76 monolayers. This is in agreement with the coverage of the p(2 × 2)-3CO structure (0.75 monolayers) determined from STM[13] and X-ray scattering.[14] Additionally, the SFG signal from the multi-coordinated CO was verified to confirm the 0.75 monolayers p(2 × 2)-3CO structure.[15] Previous studies showed that the oxidation potential of CO is also sensitive to the adsorption potential,[14] temperature,[21] and anions present in the solution.[22] Therefore, to compare a spectroscopic measurement with a CO stripping curve, it is essential to do measurements simultaneously. Since previous IRAS studies show that the intensity from atop coordinated CO is linearly proportional to CO coverage,[10] our SFG study focuses on the atop coordinated CO.

Figure 2 shows CO vibrational spectra obtained using SFG at a potential scan rate of 0.5 mV/s. All SFG spectra were taken with the ppp polarization configuration (p-polarized SFG, p-polarized visible, and p-polarized IR). The IR wavenumber was scanned from 2030 to 2110 cm^{-1} at 5 cm^{-1} intervals. Each data point in the spectra represents an average of 20 laser pulses. During a positive-going potential sweep from 0.04 to 0.8 V at 0.5 mV/s, an SFG spectrum was recorded every 22 s (equivalent to an 11 mV interval in potential). Figure 3A shows the CO stripping curve recorded during the SFG experiment. Due to a low signal-to-noise ratio, the preignition current is not visible in this measurement. However, it clearly shows that the main oxidation current peaked at 0.684 V and vanished at 0.690 V. The last SFG spectrum with observable CO intensity was recorded during the potential sweep from 0.674 to 0.685 V. There is no discrepancy between the CO stripping and the SFG signal of CO as reported in previous SFG studies.[15,16] It suggests that, in previous SFG studies, the inconsistency between SFG intensity and CO stripping curve was mostly due to the difference in scan rate used during SFG and CO stripping measurements. In those experiments, each SFG spectrum at a given potential was acquired in the 20−60 min time scale, while the CO stripping curve was measured in less than a minute.

Figure 3B shows the resonant frequency ω_q obtained by fitting the spectra with eq 1. The external potential induces changes in the vibrational frequency of the adsorbed CO molecule. This change is generally referred to as a vibrational Stark effect and is quantified by the stark tuning rate $d\omega_q/dV$.[23,24] Previous IRAS studies indicated that the stark tuning rate increases with decreasing CO coverage.[10] For potentials $V < 0.50$ V, we obtain a stark tuning rate of 29.1 ± 1.4 cm^{-1}/V. This is in agreement with Weaver's studies showing a small stark tuning rate for a CO coverage close to saturation. In Figure 3B, for potentials

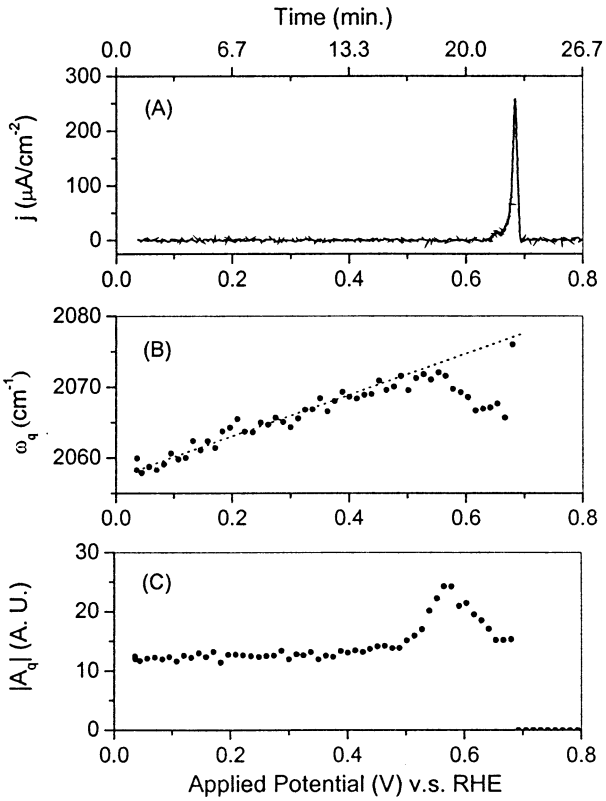

Figure 3. (A) CO stripping current measured simultaneously with SFG spectra shown in Figure 2. Label on the top indicates the time scale during the experiment. (B) and (C) CO stretching frequency and amplitude obtained by fitting the spectra in Figure 2 with eq 1. The dashed line in (B) is a linear fit with a slope of 29.1 ± 1.4 cm^{-1}/V.

0.500 V < V < 0.670 V, the frequency decreases with a slope of −48 ± 6 cm^{-1}/V when the potential increases. IRAS studies by Weaver et al. show that the frequency of CO at a fixed potential red shifts linearly with the decrease of CO coverage.[10] It suggests that the observed red shift of the frequency in the preignition region, as shown in Figure 3B, is due to the decrease of CO coverage, as indicated in Figure 1B.

A significant blue shift of the CO frequency was observed at potential V = 0.680 V during the main oxidation process. The mechanism for this blue shift is not clear. The phenomenon has not been observed by previous IRAS experiments. Although this blue shift during main oxidation is reproducible in our experiments, it is worth pointing out that the magnitude of the blue shift is uncertain. The CO stripping curves in Figure 1 show that the main oxidation occurs within a 0.05 V interval, which corresponds to 100 s in a 0.5 mV/s scan. Since the spectrum acquisition time is 22 s, which is not significantly smaller than 100 s, it can be misleading to make a quantitative conclusion based on the spectra recorded during the main oxidation process. The fitting values of width Γ in eq 1 are about 10 cm^{-1}, except for the last two spectra at 0.667 and 0.680 V, at which Γ is equal to 13 and 16 cm^{-1}, respectively. Again, one should keep in mind that a rapid frequency blue shift can behave like a broadening of the peak if the spectrum acquisition time is not significantly smaller than the time scale of the reaction.

Figure 3C shows the amplitude A_q obtained by fitting each spectrum to eq 1. The amplitude is approximately constant up to 0.5 V and then shows a 90% transient increase before the onset of oxidation. To the best of our knowledge, this is the first time this phenomenon has been observed. There are two possibilities for this transient amplitude change: a change in

the CO orientation, or a change in the hyperpolarizability of CO molecules. In the first case, the intensity of SFG is related to the average tilting angle and the angle distribution width of CO molecules, as described in eq 2. Unfortunately, the nonlinear susceptibility of CO has only two independent nonzero components, $\chi^{(2)}_{yyz} = \chi^{(2)}_{xxz}$ and $\chi^{(2)}_{zzz}$, which give two detectable SFG polarization combinations, ppp ($\chi^{(2)}_{xxz} + \chi^{(2)}_{zzz}$) and ssp ($\chi^{(2)}_{yyz}$).[15] They do not allow us to determine both the CO tilting angle and angle distribution width. Although evidence of CO tilting away from the surface normal at high coverage (>0.66 monolayers) has been observed in ultrahigh vacuum (UHV) on a Pt(111) surface by using electron stimulated desorption ion angular distribution (ESDIAD),[25] the angle distribution of CO molecules on a Pt(111) surface in aqueous solution is unknown. In the second case, a change in the hyperpolarizability of CO can also result in a change in A_q. As described in eq 3, the amplitude A_q is proportional to both the infrared dipole derivative and the Raman tensor derivative. Because the amplitude from IRAS measurements did not show similar behavior,[10] it suggests that a Raman tensor change could be responsible for the intensity change of SFG. However, SFG alone cannot conclude whether the dramatic SFG intensity change comes from the Raman tensor or the CO orientation.

It would be interesting to compare Raman intensity and SFG intensity. However, the application of Raman spectroscopy to metal−solution interfaces has suffered from low sensitivity. Currently, studies of CO oxidation on Pt electrode using Raman spectroscopy are very limited. In 1977, Cooney et al. observed a very low-intensity CO stretching mode from a platinized Pt electrode.[26] In 1990, a surface enhanced Raman scattering (SERS) spectrum was measured from CO adsorbed on Pt-coated gold electrode, but two stretching modes were observed, one of which was from the CO bound to uncovered gold substrate.[27] Recently, Tian et al. performed an SERS study using 632.8 nm excitation on a roughened Pt electrode in 0.1 M NaOH solution with a spectrum-acquisition time of 200 s.[28] In Tian's measurement, the CO stretching intensity showed a considerable increase, while the frequency red shifted from 2056 to 2041 cm^{-1}. Subsequently, the frequency increased to 2094 cm^{-1}, while the amplitude vanished due to oxidation. Although these results were qualitatively similar to the results presented here, a Raman scattering study of CO on Pt(111) would be more desirable for comparison.

Recently, inconsistencies between IR and SFG spectra were also observed from CO on Ni(111) in a UHV environment.[29] The anomalous coverage dependence of the SFG signal was ascribed to the change of the Raman tensor. As Raman spectroscopy has been hampered due to poor sensitivity and those intermediate states of CO are short-lived, SFG provides a powerful technique to study metal−liquid interfaces. Further experimental and theoretical investigation of the frequency shift and amplitude change before and during CO oxidation that was observed in the SFG spectra may reveal further information about the oxidation process.

Summary

Voltammetry studies at different potential scan rates showed that the oxidation potential of CO on a Pt(111) electrode in 0.5 M H_2SO_4 solution was lowered by 0.1 V, from 0.84 to 0.74 V, by decreasing the scan rate from 50 to 0.5 mV/s. Sum-frequency generation, CO vibrational spectra, and voltammetry were measured simultaneously to clarify the discrepancy between SFG and CO stripping measurements reported in earlier SFG studies. Our experiments showed that the SFG peak attributed to CO stretching vanished immediately after the CO stripping current reached its maximum value and that there is no discrepancy between SFG and CO stripping measurements. In the preignition potential region, the frequency shift of the CO stretching mode observed by SFG is consistent with that observed by IR spectroscopy. Additionally, in the ignition potential region, a significant frequency blue shift was observed. The amplitude change observed by SFG is significantly different from that observed by IR spectroscopy but shows similar behavior to limited Raman spectroscopy measurements obtained from a roughened Pt surface.

Acknowledgment. This work was supported by the Director, Office of Science, Office of Basic Energy Sciences, Division of Materials Sciences and Engineering, of the U.S. Department of Energy under Contract No. DE-AC03-76SF00098.

Appendix

Since water shows strong absorption in the IR region, the effect of laser heating was investigated by solving a heat diffusion equation. Because the temperature gradient in the surface normal direction is much larger than the temperature gradient in the direction parallel to surface, the heat diffusion equation was simplified to a one-dimensional equation

$$\rho C_p \frac{\partial T(z,t)}{\partial t} = Q + k\frac{\partial^2 T(z,t)}{\partial z^2}$$

where ρ, C_p, Q, and k are density, heat capacity, heat added, and thermal conductivity, respectively. The calculation showed the average temperature change of water due to laser irradiation was on the order of 1 °C.

References and Notes

(1) Kitamura, F.; Takahashi, M.; Ito, M. *Surf. Sci.* **1989**, *223*, 493.
(2) Chang, S.; Leung, L. H.; Weaver, M. J. *J. Phys. Chem.* **1989**, *93*, 5341.
(3) Zou, S.; Weaver, M. J. *J. Phys. Chem.* **1996**, *100*, 4237.
(4) Kunimatsu, K.; Gordon, W. G.; Seki, H.; et al. *Langmuir* **1985**, *1*, 245.
(5) Kunimatsu, K.; Seki, H.; Golden, W. G.; et al. *Langmuir* **1986**, *2*, 464.
(6) Kita, H.; Shimazu, K.; Kunimutsu, K. *J. Electroanal. Chem.* **1988**, *241*, 163.
(7) Lynch, M. L.; Corn, R. M. *J. Phys. Chem.* **1990**, *94*, 4382.
(8) Gutierrez, C.; Caram, J. A. *J. Electroanal. Chem.* **1991**, *308*, 321.
(9) Markovic, N. M.; Ross, P. N. *Surf. Sci. Rep.* **2002**, *45*, 121.
(10) Leung, L. W. H.; Wieckowski, A.; Weaver, M. J. *J. Phys. Chem.* **1988**, *92*, 6985.
(11) Roth, J. D.; Chang, S.; Weaver, M. J. *J. Electroanal. Chem.* **1990**, *288*, 285.
(12) Ocko, B.; Wang, B. M. *Phys. Rev. Lett.* **1990**, *65*, 1466.
(13) Villegas, I.; Weaver, J. M. *J. Chem. Phys.* **1994**, *101*, 1648.
(14) Markovic, N. M.; Grgur, B. N.; Lucas, C. A.; et al. *J. Phys. Chem. B* **1999**, *103*, 487.
(15) Baldelli, S.; Markovic, N.; Ross, P.; et al. *J. Phys. Chem. B* **1999**, *103*, 8920.
(16) Dederichs, F.; Friedrich, K. A.; Daum, W. *J. Phys. Chem. B* **2000**, *104*, 6626.
(17) Clavilier, J.; Faure, R.; Guinet, G.; et al. *J. Electroanal. Chem.* **1980**, *107*, 205.
(18) Clavilier, J.; Achi, K. E.; Petit, M.; et al. *J. Electroanal. Chem.* **1990**, *295*, 333.
(19) Shen, Y. R. *Rev. Phys. Chem.* **1989**, *40*, 327.
(20) Ikezawa, Y.; Saito, H.; Fujisawa, H.; et al. *J. Electroanal. Chem.* **1988**, *240*, 281.

(21) Markovic, N. M.; Schmidt, T. J.; Grgur, B. N.; et al. *J. Phys. Chem. B* **1999**, *103*, 8568.
(22) Markovic, N. M.; Lucas, C. A.; Rodes, A.; et al. *Surf. Sci*. **2002**, *499*, L149.
(23) Bishop, D. M. *Rev. Mod. Phys.* **1990**, *62*, 343.
(24) Lambert, D. K. *Electrochim. Acta* **1996**, *41*, 623.
(25) Kiskinova, M.; Szabo, A.; Yates, J. T. *Surf. Sci*. **1988**, *205*, 215.
(26) Cooney, R. P.; Fleischmann, M.; Hendra, P. J. *J. Chem. Soc., Chem. Commun.* **1977**, *235*.
(27) Zhang, Y.; Weaver, M. J. *Langmuir* **1993**, *9*, 1397.
(28) Tain, Z. Q.; Ren, B.; Mao, B. W. *J. Phys. Chem. B* **1996**, *101*, 1338.
(29) Katano, S.; Bandara, A.; Kubota, J.; et al. *Surf. Sci*. **1999**, *427*, 337.